Separate Power Allocation and Control Method Based on Multiple Power Channels for Wireless Power Transfer

Yongcan Huang, *Student Member, IEEE*, Chunhua Liu, *Senior Member, IEEE*, Yang Xiao, *Student Member, IEEE*, and Senyi Liu, *Student Member, IEEE*

***Abstract*—Most of the existing one-to-multiple wireless power transfer systems are single-channel one-to-multiple wireless power transfer (SOWPT) systems. They only utilize one power channel to charge multiple receivers. In this article, a novel multichannel one-to-multiple wireless power transfer (MOWPT) system is proposed, which can deliver power to different receivers simultaneously with separate power channels. In the proposed MOWPT system, the composited compensation topology is utilized to build multiple power channels, which possess totally different resonant frequencies and nearly do not affect each other. Compared with those existing SOWPT systems, the power of receivers of the proposed MOWPT system can be simply and separately controlled by changing the duty cycles of the inverters without a complex control method and extra dc–dc converters. In order to analyze the performances of the proposed MOWPT system, a 0-*LC* MOWPT system, which utilizes the air transformers to provide multiple power supplies of different frequencies, is modeled and analyzed in detail. Moreover, based on the analysis results, a corresponding parameter design method is proposed to simplify the design procedure of this MOWPT system. Finally, an experimental prototype is built up to verify the performances of the proposed MOWPT system and the parameter design method.**

***Index Terms*—*LCL* compensation topology, multiple power channels, power allocation, wireless power transfer (WPT).**

I. Introduction

WIRELESS power transfer (WPT) technology has been widely used in industry and home appliances for safety and convenience [1], [2]. With the increasing commercialization of the medium- and small-power WPT system, utilizing one transmitter to charge multiple receivers has attracted more and more attention [3]–[5]. In addition, one-to-multiple wireless power transfer (OWPT) technology has been introduced on wireless charging for various medium- and small-power mobile devices because it can directly decrease the cost of building transmitters [6].

The OWPT systems can be classified into two types according to their different characteristics and control methods. The first type of OWPT system utilizes the impedance transformation of the dc–dc modules to allocate the power to the different load receivers [6]–[8]. The second type of OWPT system utilizes the different frequency characteristics of receivers [9]–[13]. For the first type of OWPT system, the power can be accurately allocated to the load receivers according to their requirements. Then, the zero-voltage switching can be realized easily. But the extra dc–dc modules will result in the unexpected power loss, which will further decrease the transfer efficiency. Besides, the more serious problem of this method is that the realization of the precise power allocation of receivers relies on the cooperation of all dc–dc converters. It means that the control method will be relatively complex. On the other hand, for the second type of the OWPT system, the control method and circuit could be relatively simple. However, soft switching is difficult to be achieved for both the power supplies while the transmitter is simultaneously charging the multiple receivers at the rated power.

Most of the second type of the OWPT systems are single-channel one-to-multiple wireless power transfer (SOWPT) systems. The SOWPT system cannot charge all receivers in max power simultaneously because only one power channel can be built for a specific period of time. In [9] and [10], the transmitter of the SOWPT system alternately works at different frequencies for a period of time. Thus, for a specific period of time, only one receiver can get enough power from the transmitter because the impedances of other receivers are mismatched. In [11] and [12], a multifrequency superposition methodology is proposed, which superimposes multiple powers with different resonant frequencies in the same transmitter. However, the transmitter can only work alternately at different resonant frequencies to charge different types of receivers. Thus, their receivers cannot achieve the expected power simultaneously. Besides, the transformers used in these articles are not analyzed, which actually have a big impact on the resonance of the whole system. In [13], a dual-band wireless power system is proposed, which can simultaneously charge two receivers by using an

Manuscript received August 24, 2019; revised November 18, 2019; accepted February 4, 2020. Date of publication February 12, 2020; date of current version May 1, 2020. This work was supported in part by a grant from the Science Technology and Innovation Committee of Shenzhen Municipality, Shenzhen, China, under Project JCYJ20180307123918658, in part by a grant from the Innovation and Technology Commission, Hong Kong, under Project ITP/027/19AP, in part by the Teaching Development Grant and City Strategic Research Grant from the City University of Hong Kong, Hong Kong, under Projects TDG6000675, SRG11218317, and SRG11218519. Recommended for publication by Associate Editor M. Vitelli. *(Corresponding author: Chunhua Liu.)*

The authors are with the School of Energy and Environment, City University of Hong Kong, Hong Kong, and also with the Shenzhen Research Institute, City University of Hong Kong, Shenzhen 518000, China (e-mail: yongcan.huang@my.cityu.edu.hk; chunliu@cityu.edu.hk; ansel.shaw@my.cityu.edu.hk; senyiliu2-c@my.cityu.edu.hk).

Color versions of one or more of the figures in this article are available online at https://ieeexplore.ieee.org.

Digital Object Identifier 10.1109/TPEL.2020.2973465

improved Class-E converter. However, the number of receivers is limited, and the control method is relatively complex. In [14], a multiple-to-multiple WPT system is proposed, which can simultaneously allocate power to different receivers. But there are so many transmitters that need to be arranged in practical applications and the circuit of the whole primary side of the WPT system is complex. In [15], a multifrequency multipower one-to-many WPT system is proposed. But this system needs to work at a time-sharing mode to allocate power to receivers. In [16], a multiple outputs WPT system for electric vehicles is proposed, which also works at the time-sharing mode. In [17], the frequency bifurcation is utilized to simultaneously charge many loads. However, although the frequency bifurcation can be used to select and charge suitable receivers, the transmitter still works in a time-sharing way, which means the fully simultaneous charging still cannot be realized. In summary, many attempts have been made to transfer more power to different loads simultaneously. But these attempts make the topology and the corresponding control methods more complex. Actually, there is still a lack of fully simultaneous charging technology.

In this article, a new multichannel one-to-multiple WPT (MOWPT) system is proposed, which can overcome the above-mentioned problems. The proposed system is especially useful to charge the devices of different power levels in the same zone, such as the mixed parking area of electric vehicles (EVs) and electric bicycles, the smart kitchen with many different electric appliances, and the human body with different charging-level microrobots, as well as the occasion with different charging-pattern devices. In such mentioned WPT systems, building too many transmitters will lead to extremely high cost and great inconvenience. Thus, in these emerging applications, with the proposed MOWPT system, the power of the source can be simultaneously transferred to the different devices under different power levels through different power channels without complicated control strategies. The proposed idea is full of great potential for practical applications.

The key work and contributions of this article are listed as follows. First, recent works related to the OWPT system are analyzed and summarized. To make the results clear, based on the experimental results, a comparison table is given in Section V, which shows the advantages of this work. Second, the composite compensation topology based on the *LCL* topology, which has more than two natural resonant frequencies, is utilized to construct multiple power channels. Third, based on the fundamental harmonic analysis (FHA) method, the basic MOWPT system is modeled, and the two air transformers are also taken into consideration. Third, the transmitter characteristics of the basic MOWPT system with two different receivers are investigated. The analysis results show that there are multiple resonant angle frequencies that can be used to construct the corresponding power channels for different receivers. When compared with the method in [11] and [17], the circuit of the proposed MOWPT system is much simpler. This is because the practical MOWPT with two channels only needs one extra coil, which can even be replaced by the secondary sides of transformers in series. Moreover, the control method is simpler when compared with the above-mentioned methods. The power channels have totally different resonant frequencies and almost do not affect each other. It means that the power of receivers can be adjusted separately by simply changing the duty cycles of inverters. Fourth, a practical system design method is elaborated and then an experimental prototype is designed based on the proposed method. Finally, the designed experimental prototype is built up. The experimental results are given to verify the validity of the performances of the proposed MOWPT system and the parameter design method.

II. Proposed MOWPT System

The proposed OWPT system with multiple power channels is proposed, as shown in Fig. 1. This system has multiple different half-bridge converters to provide the power of different frequencies. The *LCL* topology is utilized as the basic compensation topology of the transmitter, which can provide two natural resonant frequencies to construct two energy channels. The series *LC* section can be added to the basic *LCL* topology to provide more resonant points. All receivers are coupled with the same transformer coil to get the power simultaneously. Then, the conventional uncontrollable rectifiers and filter capacitors are used to convert ac–dc for loads.

In Fig. 1, L_i and C_i are the inductance and capacitance of the *i*th *LC* circuit. For the transmitter, L_{series} is the first inductance of the basic *LCL* topology, C_p is the compensation capacitance of the basic *LCL* topology, and L_p is the self-inductance of the transmitter coil of the basic *LCL* topology. $L_{s1}, L_{s2}, \ldots, L_{si}$ are the self inductances of inductors of receivers. $C_{s1}, C_{s2}, \ldots, C_{si}$ are the capacitances of compensated capacitors of receivers. $R_p, R_{s1}, R_{s2}, \ldots, R_{si}$ are the equivalent series resistances of coils and they are considered to be constant in the mathematical model to simplify the analysis. $M_i\,(i = 1, 2, \ldots, n, j = 1, 2, \ldots, n)$ are the mutual inductances between the transmitter and receivers. M_{ij} are the mutual inductances among receivers.

A. Power Supply

Based on the work in [11], the air-core transformers are utilized in this article to realize the superposition of ac sources with different frequencies, which is also shown in Fig. 1. The advantages of using air-core transformer are listed as follows.

1) The secondary sides of transformers can be used as the series inductor of the basic *LCL* circuit or the series *LC* circuit, which can simplify the circuit.
2) Different power channels can be isolated, which can simplify the modeling of the whole system.
3) The power of each channel can be controlled by simply changing the duty ratios of half-bridge inverters. Thus, it is unnecessary to adjust the output power by the extra dc–dc circuits.

To properly utilize air-core transformers to supply power to the MOWPT system, the inductance L_{pi} of the primary side of air-core transformer and branch resonant capacitor C_i should satisfy (1). The parameter ω_{oi} is the switching angle frequency, which should be close to the natural angle resonant frequency ω_{si} of receivers after the parameter design

$$2\pi \frac{1}{\sqrt{L_{pi}C_i}} = \omega_{oi}. \tag{1}$$

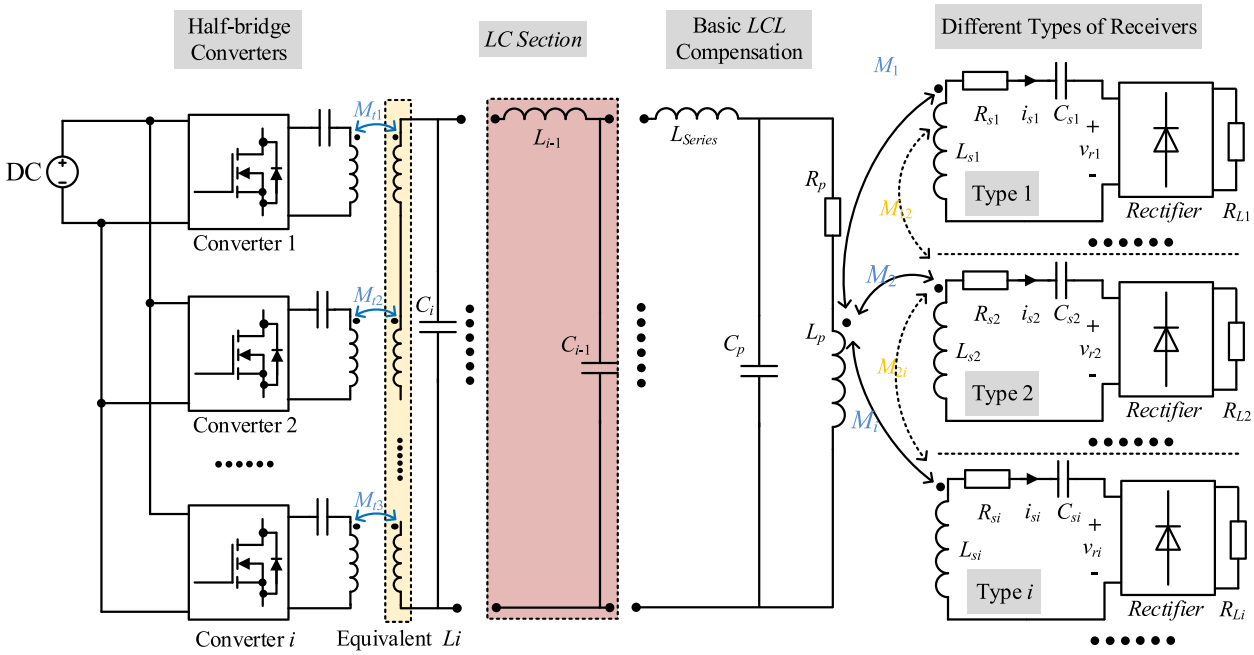

Fig. 1. Proposed MOWPT system and the power supply method by using air-core transformers.

B. Circuit of Transmitter

To transfer power to different types of receivers, the resonant topology of the transmitter should have more than one natural resonant frequency. Generally, the common series and parallel resonant topology only have one natural resonant frequency, which obviously cannot satisfy the requirement of the MOWPT system. Thus, one composite resonant topology is proposed in this article, which combines the basic *LCL* topology and several *LC* circuits in series. The circuit of the composite compensation topology is shown in Fig. 1. The *LCL* topology is necessary for the MOWPT system, which has more than two natural resonant frequencies. Among these natural resonant frequencies, there are two resonant frequencies suitable as the switching frequencies to build power channels. While the power supplies operate at the two switching frequencies, the transmitter can transfer relatively maximum power for different receivers through different power channels. Importantly, the two power channels are independent, which means the time sharing is unnecessary in the proposed MOWPT system.

Moreover, the basic *LCL* topology with *LC* circuits in series can provide more natural resonant frequencies for the MOWPT system. With the increase in the number of the *LC* circuits in series , the number of more natural resonant frequencies of the transmitter will also increase, namely, more power channels can be built to transfer energy to different types of receivers according to the requirements of the practical applications.

C. Circuit of Receivers

The receivers of the MOWPT system generally use the series circuit as the compensation topology because the series circuit has great frequency characteristics. This is different from the parallel compensative circuit of the WPT system [6]. The series compensative circuit can resonant at a fixed frequency with different resistance components, namely the resonant frequency of the series compensative circuit will be constant when its resistance component is changing. This is especially useful for the OWPT systems with varying loads or different loads in their receivers, which is able to keep the resonant frequency of systems unchanging. Besides, the reflected impedance of the series circuit is purely resistive, while the frequency of the current is equal to the natural resonant frequency, which is also helpful to initiate and design the natural frequencies of the transmitter. After the resonant circuit of each receiver, an uncontrollable rectifier is connected in series, which can change the ac–dc for the load.

The main advantage of the MOWPT system is that there are no dc–dc circuits in the receivers to allocate the output powers among the loads. The power of each channel can be adjusted by changing the duty cycle of the corresponding converter.

III. Mathematical Model of Proposed 0-*LC* MOWPT

Generally, the circuit of the transmitter of the proposed system includes several *LC* circuits to provide more resonant frequencies to build the power channels, namely the "n-*LC*". The "0-*LC*" means that there are no more *LC* circuits connected in series before the basic *LCL* circuit of the transmitter. In this article, the 0-*LC* MOWPT system is used as a presentative example for simplifying the theoretical analysis in which the circuit and model are shown in Fig. 2(a) and (b). As mentioned above, the FHA method is adopted to analyze the steady state of the 0-*LC* MOWPT system, which is based on the high-quality factors of resonant tanks. In Fig. 2(b), U_1 and U_2 denote the input ac voltages, whose frequencies are different. $I_{\text{in}(i)}$, $I_{p(_i)}$, $I_{s1(i)}$, and $I_{s2(i)}$ are the input current, the current of transmitter, and

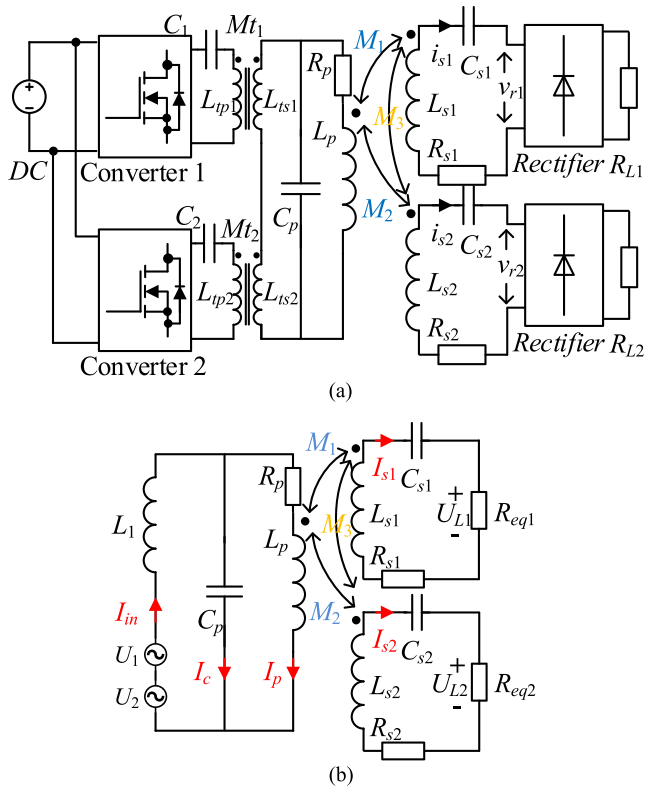

Fig. 2. Circuit and model of the 0-*LC* MOWPT system.

the currents of receivers, respectively, where i in the brackets means at a certain switching frequency f_i ($i = 1$ or 2).

Due to the half-bridge configuration utilized in this circuit, the norms of U_1 and U_2 can be calculated as follows [11], [18], [19]:

$$U_1 = \frac{\sqrt{2}\sin(D_1\pi)}{\pi}U_{\mathrm{DC}}, \quad U_2 = \frac{\sqrt{2}\sin(D_2\pi)}{\pi}U_{\mathrm{DC}} \tag{2}$$

where D_1 and D_2 are the duty cycles of converters.

Besides, the equivalent loads R_{eq1} and R_{eq2} can be calculated as follows [11], [18], [19]:

$$R_{\mathrm{eq1}} = \frac{8}{\pi^2}R_{L1}, \quad R_{\mathrm{eq2}} = \frac{8}{\pi^2}R_{L2}. \tag{3}$$

Then, according to KVL and KCL, the matrix of the model can be given as follows:

$$\begin{bmatrix} U_i \\ 0 \\ 0 \\ 0 \end{bmatrix} = \begin{bmatrix} Z_{\mathrm{in(i)}} & \frac{j}{C_p\omega_i} & 0 & 0 \\ \frac{j}{C_p\omega_i} & Z_{p(i)} & -j\omega_i M_1 & -j\omega_i M_2 \\ 0 & -j\omega_i M_1 & Z_{s1(i)} & j\omega_i M_3 \\ 0 & -j\omega_i M_2 & j\omega_i M_3 & Z_{s2(i)} \end{bmatrix} \begin{bmatrix} I_{in(i)} \\ I_{p(i)} \\ I_{s1(i)} \\ I_{s2(i)} \end{bmatrix} \tag{4}$$

where

$$\begin{cases} Z_{\mathrm{in(i)}} = j\omega_i L_1 + R_1 + \frac{1}{j\omega_i C_p} + \sum\limits_{j\neq i} Z_{trj} \\ Z_{p(i)} = j\omega_i L_p + R_p + \frac{1}{j\omega_i C_p} \\ Z_{s1(i)} = j\omega_i L_{s1} + R_{s1} + \frac{1}{j\omega_i C_{s1}} + R_{L1} \\ Z_{s2(i)} = j\omega_i L_{s2} + R_{s2} + \frac{1}{j\omega_i C_{s2}} + R_{L2}. \end{cases}$$

By solving (4), the currents can be obtained from (5) shown at the bottom of this page, which are shown in the following text. Moreover, the powers and efficiency can be calculated by combining (5) and (6) while the two power channels work simultaneously

$$P_{L1} = \sum_{i=1}^{2} \left|I_{s1(i)}\right|^2 R_{\mathrm{eq1}}, \quad P_{L2} = \sum_{i=1}^{2} \left|I_{s2(i)}\right|^2 R_{\mathrm{eq2}}$$

$$\eta = \frac{P_{L1} + P_{L2}}{P_{\mathrm{in1}} + P_{\mathrm{in2}}}. \tag{6}$$

From (1) to (6), it can be seen that the characteristics of the 0-*LC* MOWPT are difficult to be directly analyzed. Thus, in Section IV, the receivers of the 0-*LC* MOWPT system will be analyzed first. Then, based on the analyzed results, the transmitter will be deeply explored. Meanwhile, the parameter design method will be given based on the analysis conclusions.

IV. Analysis of Power Channels

To further reveal the characteristics of the 0-*LC* MOWPT system, especially the frequency characteristic, the system will be analyzed in two steps. In the first step, the two receivers and their reflected impedances are analyzed at different operating frequencies. Then, the transmitter will be analyzed based on the analysis results of the receivers.

$$I_{in(i)} = \frac{U_i\left(C_p^2 Z_{p(i)} Z_{s1(i)} Z_{s2(i)}\omega_i^2 + C_p^2 M_3^2 Z_{p(i)}\omega_i^4 + C_p^2 M_2^2 Z_{s1(i)}\omega_i^4 + C_p^2 M_1^2 Z_{s2(i)}\omega_i^4 - 2jC_p^2 M_1 M_2 M_3\omega_i^5\right)}{Z_{s1(i)} Z_{s2(i)} + M_3^2\omega_i^2 + C_p^2 Z_{\mathrm{in}(i)} Z_{p(i)} Z_{s1(i)} Z_{s2(i)}\omega_i^2 + C_p^2 M_{3\mathrm{in}(i)}^2 Z_{p(i)}\omega_i^4 + C_p^2 M_2^2 Z_{\mathrm{in}(i)} Z_{s1(i)}\omega_i^4 + C_p^2 M_1^2 Z_{\mathrm{in}(i)} Z_{s2(i)}\omega_i^4 - 2jC_p^2 M_1 M_2 M_3 Z_{\mathrm{in}(i)}\omega_i^5}$$

$$I_{p(i)} = -\frac{jC_p U_i\omega_1\left(Z_{s1(i)} Z_{s2(i)} + M_3^2\omega_1^2\right)}{Z_{s1(i)} Z_{s2(i)} + M_3^2\omega_i^2 + C_p^2 Z_{\mathrm{in}(i)} Z_{p(i)} Z_{s1(i)} Z_{s2(i)}\omega_i^2 + C_p^2 M_3^2 Z_{\mathrm{in}(i)} Z_{p(i)}\omega_i^4 + C_p^2 M_2^2 Z_{\mathrm{in}(i)} Z_{s1(i)}\omega_i^4 + C_p^2 M_1^2 Z_{\mathrm{in}(i)} Z_{s2(i)}\omega_i^4 - 2jC_p^2 M_1 M_2 M_3 Z_{\mathrm{in}(i)}\omega_i^5}$$

$$I_{s1(i)} = \frac{C_p U_i\omega_1^2\left(jM_1 Z_{s2(i)} + M_2 M_3\omega_1\right)}{jZ_{s1(i)} Z_{s2(i)} + jM_3^2\omega_i^2 + jC_p^2 Z_{\mathrm{in}(i)} Z_{p(i)} Z_{s1(i)} Z_{s2(i)}\omega_i^2 + jC_p^2 M_3^2 Z_{\mathrm{in}(i)} Z_{p(i)}\omega_i^4 + jC_p^2 M_2^2 Z_{\mathrm{in}(i)} Z_{s1(i)}\omega_i^4 + jC_p^2 M_1^2 Z_{\mathrm{in}(i)} Z_{s2(i)}\omega_i^4 + 2C_p^2 M_1 M_2 M_3 Z_{\mathrm{in}(i)}\omega_i^5}$$

$$I_{s2(i)} = \frac{C_p U_i\omega_1^2\left(jM_2 Z_{s1} + M_1 M_3\omega_1\right)}{jZ_{s1(i)} Z_{s2(i)} + jM_3^2\omega_i^2 + jC_p^2 Z_{\mathrm{in}(i)} Z_{p(i)} Z_{s1(i)} Z_{s2(i)}\omega_i^2 + jC_p^2 M_3^2 Z_{\mathrm{in}(i)} Z_{p(i)}\omega_i^4 + jC_p^2 M_2^2 Z_{\mathrm{in}(i)} Z_{s1(i)}\omega_i^4 + jC_p^2 M_1^2 Z_{\mathrm{in}(i)} Z_{s2(i)}\omega_i^4 + 2C_p^2 M_1 M_2 M_3 Z_{\mathrm{in}(i)}\omega_i^5} \tag{5}$$

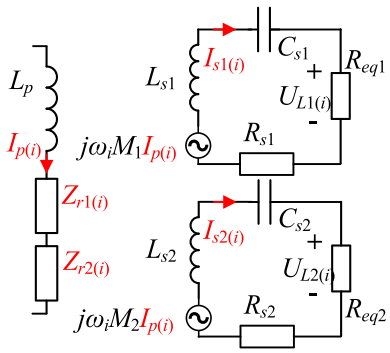

Fig. 3. Circuit of receivers for power channel *i*.

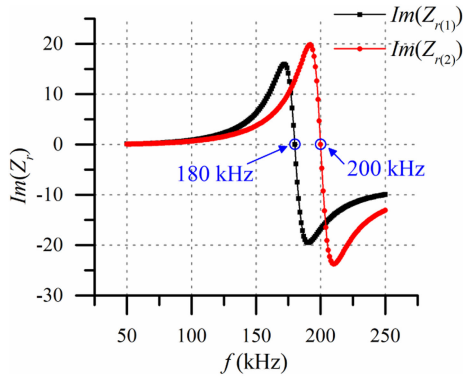

Fig. 4. Curves of the reflected reactance of two receivers.

A. Receivers and Their Reflected Impedances

The circuit of the receivers is shown in Fig. 3. At a certain operating frequency f_1 or f_2, the two receivers will get the amount of power from the transmitter. At the same time, for power channel i, the receivers will have reflected impedances $Z_{r1(i)}$ and $Z_{r2(i)}$ in the transmitter coil, which are only related to the parameters of the circuits of receivers. The equations of $Z_{r1(i)}$ and $Z_{r2(i)}$ can be obtained as (7).

When the alternating frequency f_1 of the first ac power satisfies (7), the $Z_{r1(1)}$ will be a purely resistive load and $Z_{r2(1)}$ will be an inductive or capacitive load. Also, when the frequency of the secondary ac power satisfies (7), the $Z_{r1(2)}$ will be an inductive or capacitive load and $Z_{r2(2)}$ will be a purely resistive load

$$\begin{aligned} Z_{r1(i)} &= \frac{\omega_i^2 M_1^2}{Z_{s(i)}} = \frac{\omega_i^2 M_1^2}{\frac{1}{j\omega_i C_{s1}} + j\omega_i L_{s1} + R_{s1} + R_{\mathrm{eq1}}} \\ Z_{r2(i)} &= \frac{\omega_i^2 M_2^2}{Z_{s(i)}} = \frac{\omega_i^2 M_2^2}{\frac{1}{j\omega_i C_{s2}} + j\omega_i L_{s2} + R_{s2} + R_{\mathrm{eq2}}} \end{aligned} \tag{7}$$

$$\begin{aligned} \omega_1 &= 2\pi f_{s1} = \frac{2\pi}{\sqrt{L_{s1} C_{s1}}} \\ \omega_2 &= 2\pi f_{s2} = \frac{2\pi}{\sqrt{L_{s2} C_{s2}}}. \end{aligned} \tag{8}$$

By substituting (8) into (7), the equations of reflected impedances can be simplified as follows:

$$\begin{cases} Z_{r1(1)} = \frac{\omega_1^2 M_1^2}{R_{s1}+R_{\mathrm{eq1}}}, \quad Z_{r2(1)} = \frac{\omega_1^2 M_2^2}{\frac{1}{j\omega_1 C_{s2}} + j\omega_1 L_{s2} + R_{s2} + R_{\mathrm{eq2}}} \\ Z_{r1(2)} = \frac{\omega_2^2 M_1^2}{\frac{1}{j\omega_2 C_{s1}} + j\omega_2 L_{s1} + R_{s1} + R_{\mathrm{eq1}}}, \quad Z_{r2(2)} = \frac{\omega_2^2 M_2^2}{R_{s2}+R_{\mathrm{eq2}}} \end{cases} \tag{9}$$

$$\begin{cases} Z_{r(1)} = \frac{\omega_1^2 M_1^2}{R_{s1}+R_{\mathrm{eq1}}} + \frac{\omega_1^2 M_2^2}{\frac{1}{j\omega_1 C_{s2}} + j\omega_1 L_{s2} + R_{s2} + R_{\mathrm{eq2}}} \\ Z_{r(2)} = \frac{\omega_2^2 M_1^2}{\frac{1}{j\omega_2 C_{s1}} + j\omega_2 L_{s1} + R_{s1} + R_{\mathrm{eq1}}} + \frac{\omega_2^2 M_2^2}{R_{s2}+R_{\mathrm{eq2}}}. \end{cases} \tag{10}$$

Besides, the total reflected impedance of the two receivers can be obtained from (10) at different switching frequencies.

To find the resonant frequencies of the whole reflected impedance of receivers, the imaginary part of every $Z_{r(i)}$ should be close to zero. Those found resonant frequencies can be used to set the power channels of the transmitter. Fig. 4 illustrates the curves of the reflected reactance of two receivers as functions of switching frequency. The specifications are listed as follows: $L_{s1} = L_{s2} = 50\,\mu$H; $C_{s1} = 15.64$ nF; $C_{s2} = 10.47$ nF; $R_{\mathrm{eq1}} = R_{\mathrm{eq2}} = 5.674\,\Omega$; $R_{s1} = R_{s2} = 0.03\,\Omega$; $M_1 = M_2 = 12.5\,\mu$H; and $M_3 = 2.25\,\mu$H. It can be noted that when one reflected reactance equals to 0, the other one can be relatively large. So, for one ac power, there is only one receiver that can get enough power. If two receivers want to get power simultaneously, two different ac power with corresponding switching frequencies are necessary. Moreover, the transmitter should provide multiple power channels to transfer the power with different frequencies.

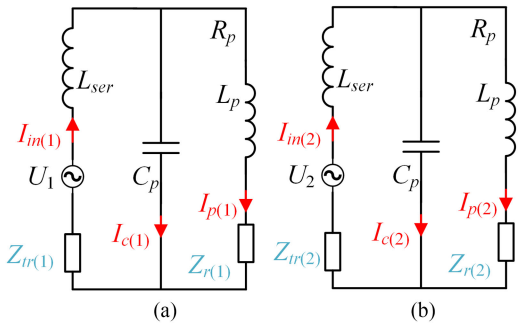

Fig. 5. Equivalent circuit of the proposed 0-*LC* MOWPT system for each power channel.

B. Transmitter With Its Resonant Frequencies

The equivalent circuit of the transmitter of the proposed 0-*LC* MOWPT system is illustrated in Fig. 5. Fig. 5(a) is for the power channel 1 and Fig. 5(b) is for the power channel 2. Each represents the transmitter that is driven by one ac source in the proposed system. Thus, only one of them will be analyzed because they share the same circuit structure. To simplify the analysis, the loss resistances of inductors are ignored.

The input impedance Z_{in} of the transmitter for ac source i can be given as follows:

$$Z_{\mathrm{in}(i)} = j\omega_i L_{\mathrm{ser}} + Z_{tr(i)} + \frac{1}{j\omega_i C_p + \frac{1}{j\omega_i L_p + Z_{r(i)}}}, \quad i = 1 \text{ or } 2 \tag{11}$$

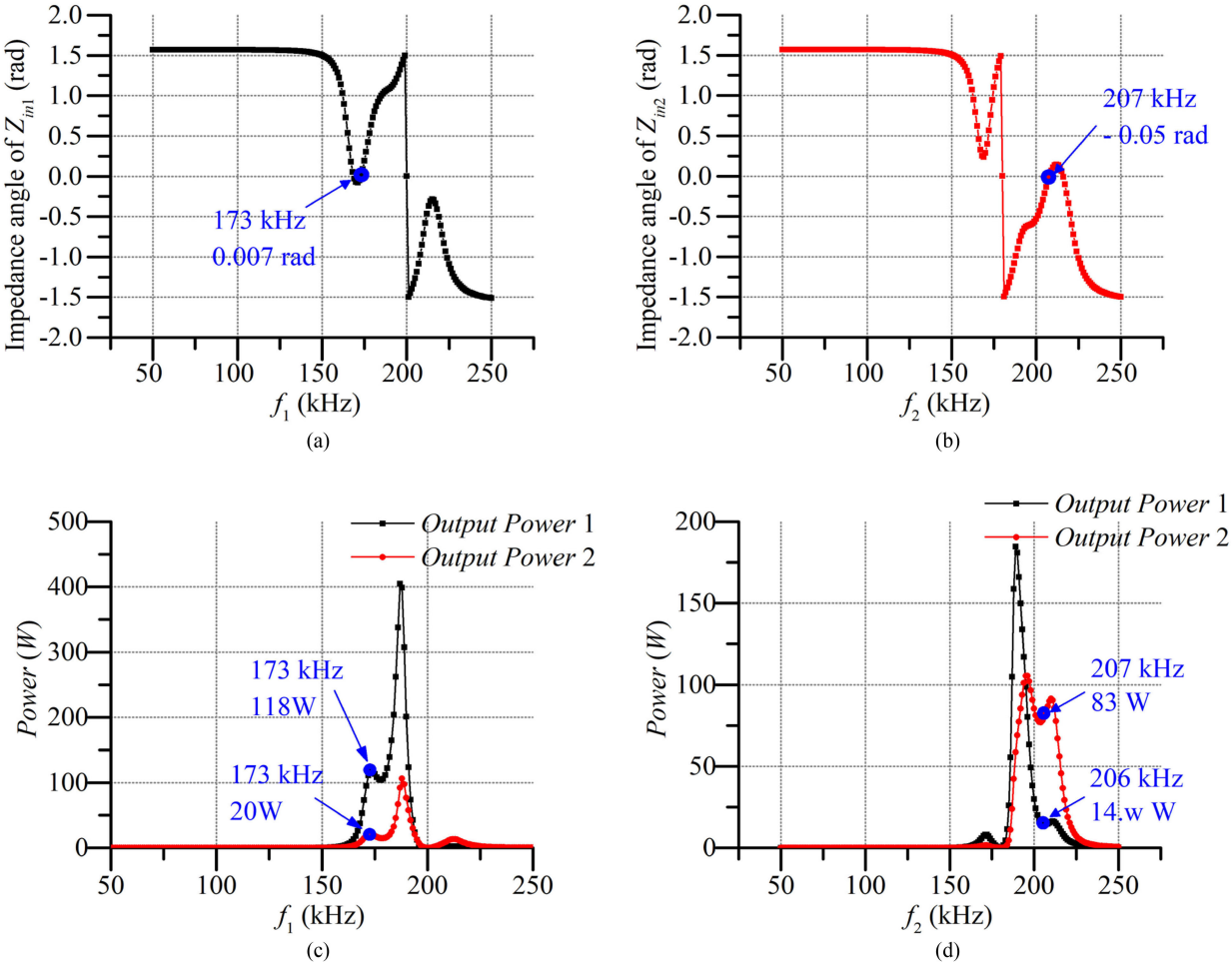

Fig. 6. (a) Impedance angle of the input impedance. (b) Sweeping result of output powers for the power source 1. (c) Impedance angle of the input impedance $Z_{\text{in}2}$. (d) Sweeping result of output powers for the power source 2.

where

$$Z_{tr(i)} = \frac{\omega_i M_{tr(j)}}{j\omega_i L_{\text{pri}(j)} + \frac{1}{j\omega_i C_j}}, \quad i = 1 \text{ or } 2,\ j \neq i. \tag{12}$$

By decomposing it into imaginary and real parts, the Z_{in} can be expressed as (13), shown at the bottom of the next page.

To realize zero phase angle (ZPA) and zero-current switching (ZCS) operation, the imaginary part of Z_{in} should be set to zero. Generally, the parameters L_p, L_{ser}, L_{s1}, L_{s2}, C_{s1}, C_{s2}, R_{equ1}, and R_{equ2} are fixed for the limited space of the practical application. So, the compensation capacitor C_p of the transmitter will be used as the variable in this article to realize ZPA and ZCS operation.

Generally, the resonant frequencies can be obtained by solving (14), shown at the bottom of the next page. However, it is hard to get analytical solutions because the order of (14) is high. Besides, the $Z_{\text{ref}(i)}$ and $Z_{tr(i)}$ are related to the resonant angle frequency ω_i, which means (14) is an implicit function of resonant angle frequency ω_i and the analytical solutions of (14) are useless. Thus, instead of the analytical solutions, combined with the formula in (14), the numerical solutions are used to find the ZPA points.

Except the parameters of receivers, the specifications of the transmitter and the air-core transformers are listed as follows: $L_p = 50\,\mu$H; $C_p = 7.8\,n$F; $L_{\text{ser}} = 100\ \mu$H; $L_{\text{sec1}} = L_{\text{sec2}} = 50\,\mu$H; $R_{\text{eq1}} = 5.674\,\Omega$; $R_{\text{eq2}} = 5.674\,\Omega$; $L_{\text{pri1}} = L_{\text{pri2}} = 50\,\mu$H; $R_{s1} = 0.1\,\Omega$; $R_{s2} = 0.1\,\Omega$; and $M_{tr1} = M_{tr2} = 4.25\,\mu$H. All the parameters are manually designed by the method proposed in the Section IV-C.

Fig. 6(a) shows the impedance angle of the input impedance $Z_{\text{in}1}$. Fig. 6(b) shows the sweeping result of output powers for the first power source. It can be seen that when the impedance angle of the input impedance closes to zero, the output power of the load 1 is much larger than the output power of the load 2. The switching frequency f_1 of the first power source is also close to the natural resonant frequency f_{s1}, which means the received reactive power of the first receiver is small. Besides, Fig. 6(c) shows the impedance angle of the input impedance $Z_{\text{in}2}$, and Fig. 6(d) shows the sweeping result of output powers for the power source 2. When the switching frequency f_2 of the second power source is 206 kHz, which is close to the natural frequency of the second receiver, the ZPA operation of the second power channel can be realized. Furthermore, the output power of the load 2 is much larger than the output power of load 1, which

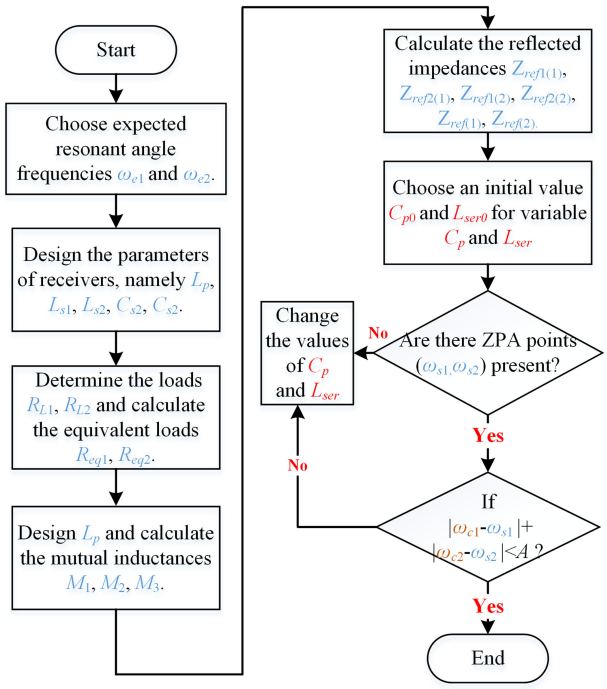

Fig. 7. Flowchart of the proposed parameter design method.

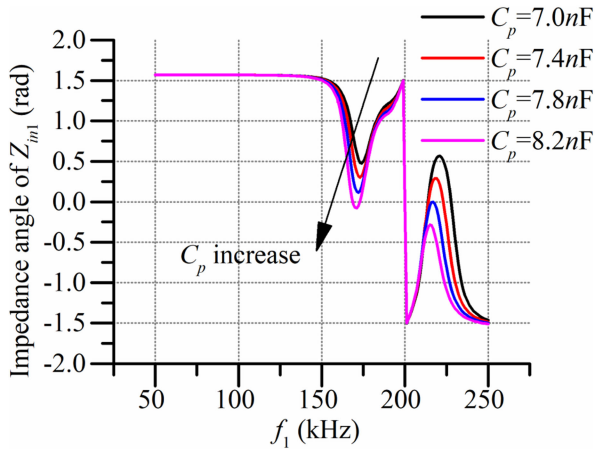

Fig. 8. Impedance angle of $Z_{\text{in}1}$ for different C_p.

means most of the input power of the source 2 is received by the second receiver.

From Fig. 6(a)–(d), it can be seen that the ZPA points of both two power sources are not the maximum power points and the ratios of $P_{\text{o}1(1)}$ to $P_{\text{o}2(1)}$ and $P_{\text{o}2(2)}$ to $P_{\text{o}1(2)}$ are also not the best. Actually, this 0-*LC* WPT system can further optimized be by replacing the manual design with some optimization algorithms, such as the genetic algorithm.

C. *Method of Parameters Design for 0-*LC *MOWPT System*

In this section, an iterative design method is proposed to design and optimize the 0-*LC* MOWPT system. The flowchart of the proposed parameter design method is shown in Fig. 7. First, the expected resonant angle frequencies ω_{e1} and ω_{e2} should be decided, which also are the expected switching angle frequencies of half-bridge inverters and the natural resonant angle frequencies of receivers ω_{s1} and ω_{s2}. Then, the parameters L_{s1}, L_{s2}, C_{s1}, and C_{s2} of receivers should be designed according to the physical requirements, such as the size of devices. Also, the loads R_{L1} and R_{L2} should be determined to calculate the equivalent loads $R_{\text{eq}1}$ and $R_{\text{eq}2}$. Then, the inductance of the transmitter coil L_p should be determined. After the transmitter and receivers are placed suitably, the mutual inductances M_1, M_2, and M_3 can be measured by the *LCR* meter.

With the above parameters, the reflected impedances of receivers can be obtained. Then, the initial values of variable C_p and L_{ser} could be decided by the designer. At this point, the parameters selection is finished. With all parameters, the impedance of each power source can be calculated by (13). Then, it can be seen that whether there are angle frequencies of suitable ZPA points. However, if the angle frequencies cannot be found by the existing parameters, the variables C_p and L_{ser} should be

$$Z_{\text{in}(i)} = \text{Re}\left(Z_{tr(i)}\right) + \frac{\text{Re}\left(Z_{r(i)}\right)}{\left(\left(\text{Re}\left(Z_{r(i)}\right)\right)^2+\left(L_p\omega_i+\text{Im}\left(Z_{r(i)}\right)\right)^2\right)\left(\frac{\text{Re}\left(Z_{r(i)}\right)^2}{\left(\left(\text{Re}\left(Z_{r(i)}\right)\right)^2+\left(L_p\omega_i+\text{Im}\left(Z_{r(i)}\right)\right)^2\right)^2}+\left(\omega_i C_p-\frac{L_p\omega_i+\text{Im}\left(Z_{r(i)}\right)}{\left(\text{Re}\left(Z_{r(i)}\right)\right)^2+\left(L_p\omega_i+\text{Im}\left(Z_{r(i)}\right)\right)^2}\right)^2\right)} + j\left(\omega_i L_{\text{ser}}+\text{Im}\left(Z_{tr(i)}\right)-\frac{\omega_i C_p-\frac{L_p\omega_i+\text{Im}\left(Z_{r(i)}\right)}{\left(\text{Re}\left(Z_{r(i)}\right)\right)^2+\left(L_p\omega_i+\text{Im}\left(Z_{r(i)}\right)\right)^2}}{\left(\frac{\text{Re}\left(Z_{r(i)}\right)^2}{\left(\left(\text{Re}\left(Z_{r(i)}\right)\right)^2+\left(L_p\omega_i+\text{Im}\left(Z_{r(i)}\right)\right)^2\right)^2}+\left(\omega_i C_p-\frac{L_p\omega_i+\text{Im}\left(Z_{r(i)}\right)}{\left(\text{Re}\left(Z_{r(i)}\right)\right)^2+\left(L_p\omega_i+\text{Im}\left(Z_{r(i)}\right)\right)^2}\right)^2\right)}\right) \tag{13}$$

$$\omega_i L_{\text{ser}}+\text{Im}\left(Z_{tr(i)}\right)-\frac{\omega_i C_p-\frac{L_p\omega_i+\text{Im}\left(Z_{r(i)}\right)}{\left(\text{Re}\left(Z_{r(i)}\right)\right)^2+\left(L_p\omega_i+\text{Im}\left(Z_{r(i)}\right)\right)^2}}{\left(\frac{\text{Re}\left(Z_{r(i)}\right)^2}{\left(\left(\text{Re}\left(Z_{r(i)}\right)\right)^2+\left(L_p\omega_i+\text{Im}\left(Z_{r(i)}\right)\right)^2\right)^2}+\left(\omega_i C_p-\frac{L_p\omega_i+\text{Im}\left(Z_{r(i)}\right)}{\left(\text{Re}\left(Z_{r(i)}\right)\right)^2+\left(L_p\omega_i+\text{Im}\left(Z_{r(i)}\right)\right)^2}\right)^2\right)}=0 \tag{14}$$

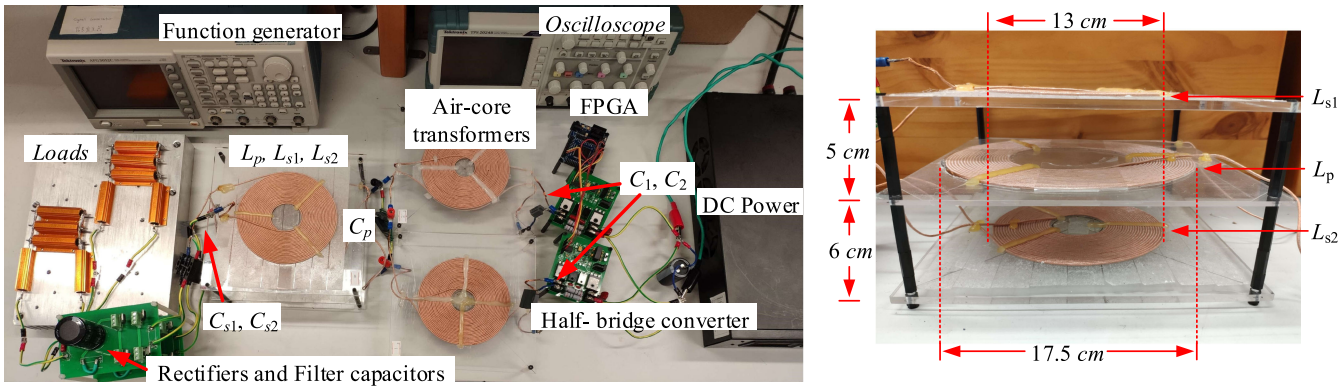

Fig. 9. Experimental prototype.

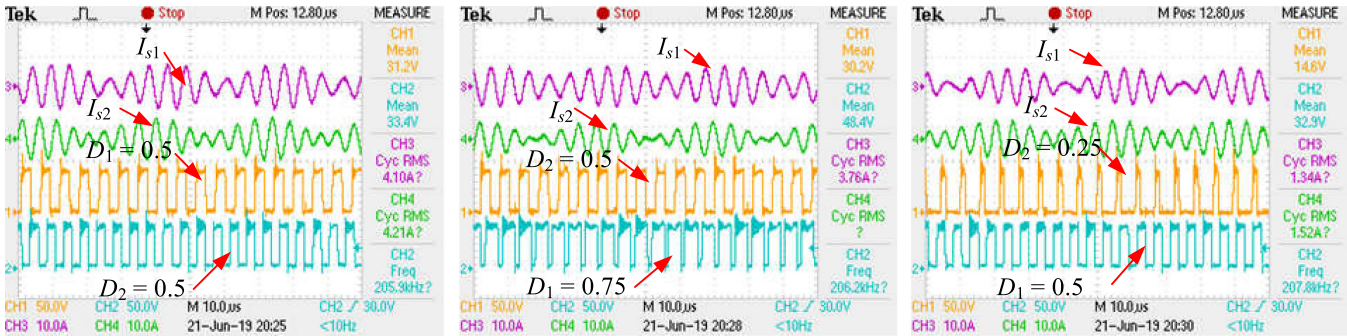

Fig. 10. Currents of receivers and corresponding duty cycles of converters. (a) $D_1 = 0.5$, $D_2 = 0.5$. (b) $D_1 = 0.5$, $D_2 = 0.75$. (c) $D_1 = 0.25$, $D_2 = 0.5$.

changed regularly to solve this issue until the suitable ω_{c1} and ω_{c2} can be found. Moreover, it is hard to make the ω_{c1} and ω_{c2} perfectly equal to the natural resonant frequencies ω_{s1} and ω_{s2}. Thus, the index named A is proposed as the acceptable index of the design, which generally is a percentage. In this article, it is chosen to be 5%. It should be noted that the parameters used in the sweeping process in Section IV-B are all manually designed with the proposed parameter design method. The process of the optimization of ω_{c1} is shown in Fig. 8. The ZPA points will occur when the C_p reach a certain value. But the ZPA points will be away from ω_{s1} with the continuous increase of C_p. Thus, after making a tradeoff, the C_p is chosen as 8.2 nF in this experimental design.

V. Experimental Performances

In this section, some experiments are used to demonstrate the effectiveness of the proposed 0-*LC* MOWPT system and the corresponding parameter design method. The experimental platform is shown in Fig. 9. In this prototype, the oscilloscope and function generator have come from *Tektronix*, whose models are TPS2024B and AFG3052C. The model of MOSFET is STC3080KL and the model of field programmable gate array (FPGA) is Altera Cyclone II EP2C5T144C8. Besides, the parameters are measured by an *LCR* meter, whose model is ISO-TECH LCR 821. The parameters of this experimental prototype are given in Table I. From this table, it can be seen that the experimental parameters are different from the theoretical parameters due to the measurement error in the process of construction.

TABLE I
Experimental Specification

	Parameter	Value	Parameter	Value
Power source	ω_{o1}	176.7 kHz	U_{dc}	60 V
	ω_{o2}	206.3 kHz		
Air-core transformer	L_{tp1}	50.81 μH	L_{tp2}	50.58 μH
	L_{ts1}	50.58 μH	L_{ts2}	50.85 μH
	M_{t1}	41.55 μH	M_{t2}	40.97 μH
	C_1	16.7 nF	C_2	12.33 nF
Transmitter	L_p	87.1 μH	Cp	8.3 nF
	R_p	0.24 Ω		
Coupler	M_1	13.13 μF	M_2	13.5 μF
	M_3	2.75 μF		
Receiver	L_{s1}	50.45 μH	L_{s2}	51.1 μH
	R_{s1}	0.17 Ω	R_{s1}	0.17 Ω
	C_{s1}	14.75 nF	C_{s2}	12.15 nF
Loads	R_{L2}	7.05 Ω	R_{L2}	7.05 Ω

TABLE II
CALCULATED AND EXPERIMENTAL RESULTS

		D_1=0.5 D_2=0.5	D_1=0.5 D_2=0.75	D_1=0.25 D_2=0.5	D_1=0.25 D_2=0.75
176.7 kHz (Experiment)	U_{L1} (V)	20.4	19.7	15.1	14.2
	P_{L1} (W)	59.8	55.8	32.8	29
206.3 kHz (Experiment)	U_{L2} (V)	17.8	13.3	16.9	11.9
	P_{L2} (W)	45.6	25.4	41.1	20
176.7 kHz (Calculation)	U_{L1} (V)	21.35	20.73	15.94	15.09
	P_{L1} (W)	65.6	61.8	36.52	32.8
206.3 kHz (Calculation)	U_{L2} (V)	19.27	14.72	18.25	13.02
	P_{L2} (W)	53.44	31	47.	24.4
Currents of power source (Experiment)		2.19 A	1.91 A	1.69 A	1.09 A
Total efficiency (Experiment)		80%	71%	73%	75%

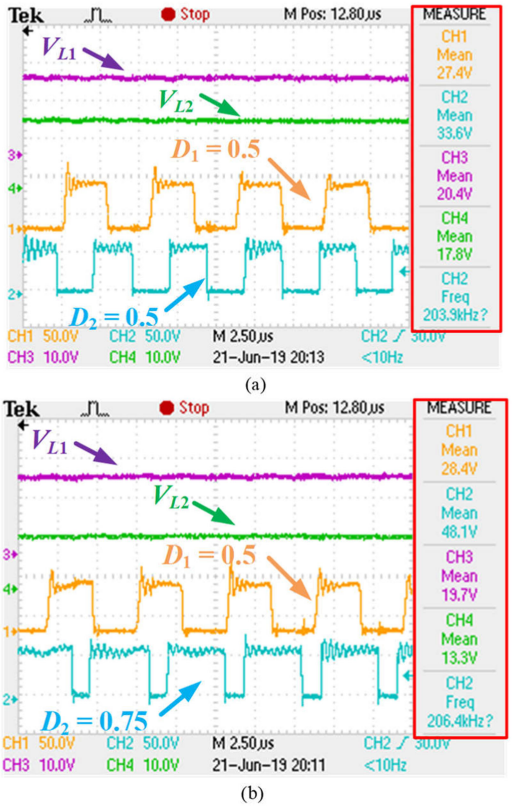

Fig. 11. Voltages of receivers and corresponding duty cycles of converters. (a) $D_1 = 0.5, D_2 = 0.5$. (b) $D_1 = 0.5, D_2 = 0.75$.

In the experiment, the whole system is an open-loop system. The whole system is controlled by changing the duty cycles of the inverters as the formula (2) without any extra circuits. Fig. 10(a)–(c) shows the currents of receivers at different duty cycles. Fig. 11(a) and (b) shows the voltages and corresponding duty cycles. Meanwhile, the data of these figures are counted in Table II with the corresponding analysis results. The efficiencies are measured from dc power to the loads and the currents of the power source are also listed in Table II.

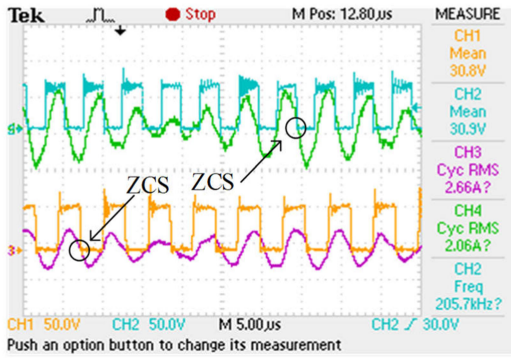

Fig. 12. Input voltages and input currents.

First, the system is initialized and the initial duty cycles of the inverters are set at 0.5. Fig. 10(a) shows the currents of receivers and the voltages of two loads are shown in Fig. 11(a). The input currents and corresponding voltages are shown in Fig. 12. It can be seen that ZCS is well realized in both channels of this system simultaneously. The whole system works as expected.

Second, the control experiment is carried out to verify the independence of power channels. When the duty cycle of one inverter is changed, the output power of the corresponding load should change accordingly, while the output power of the other load almost maintains unchanged. While the duty cycle D_1 of the first receiver changes from 0.5 to 0.25, the received power of load R_{L1} decreases from 59.8 to 32.8 W, and the received power of the load R_{L2} only changes about 5 W. The experimental results match the calculated results well. Then, the duty cycle D_2 of inverter 2 is changed. While the D_2 changes, the results are always the same. It is obvious that the 0-*LC* MOWPT system can work as expected. The difference between them is caused by the inevitable forward voltages of diodes in the rectifiers.

Third, to further verify this conclusion, as shown in Fig. 13, an fast Fourier transform (FFT) analysis is made in Simulink, where the current I_{s2}, shown in Fig. 10(a), is analyzed. From the analysis results, it can be seen that the main power obtained by receiver

TABLE III
COMPARISON RESULTS WITH REFERENCES

Reference	Number of transmitters	Number of receivers	Charging method	Control method of the power allocation (Complexity)	Extra circuit in receiver
[6]	**one**	**Multiple**	Time-sharing	\	**No**
[7]	**one**	**Multiple**	Simultaneous	No power allocation	**No**
[8]	**one**	Two	Simultaneous / Only one gets its own maximum power	Impedence transmformation (Complex)	Yes
[9]	**one**	Two/Three	Simultaneous	No power allocation	**No**
[10]	**one**	**Multiple**	Simultaneous / Only one gets its own maximum power	Coordinate control (Complex)	**No**
[11]	**one**	**Multiple**	Simultaneous / Only one gets its own maximum power	Coordinate control (Complex)	**No**
[12]	**one**	**Multiple**	Simultaneous / Only one gets its own maximum power	Coordinate control (Complex)	**No**
[13]	**one**	Two	**Simultaneous / All receivers get their own maximum power**	Separate control (Complex)	**No**
[14]	Multiple	**Multiple**	**Simultaneous / All receivers get their own maximum power**	**Separate control (Simple)**	**No**
[15]	**one**	**Multiple**	Time-sharing	\	**No**
[16]	Multiple	**Multiple**	Time-sharing	\	**No**
[17]	**Multiple (Repeater coil)**	**Multiple**	Simultaneous / Only one gets its own maximum power	\	Yes
This study	**one**	**Multiple**	**Simultaneous / All receivers get their own maximum power**	**Separate control (Simple)**	**No**

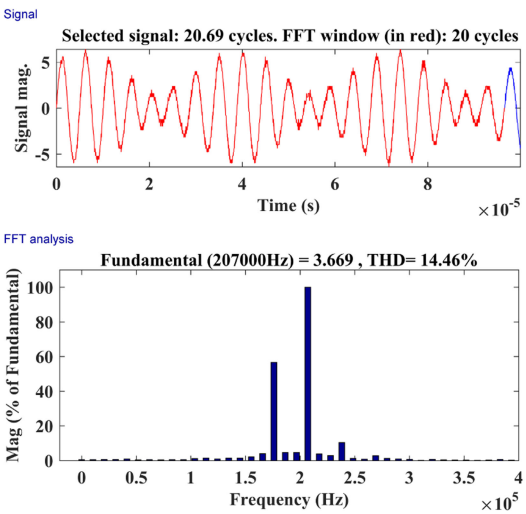

Fig. 13. FFT analysis results of I_{s2} ($D_1 = 0.5, D_2 = 0.5$).

2 is of the power 220 kHz, which can verify the above conclusion. Besides, with further optimized parameters and bigger difference between the two resonant frequencies, the receiver 2 will get less power from power channel 1. The experimental results and the FFT analysis verify the independence of power channels.

With the verified conclusions, the proposed system is compared with those systems in [6]–[17]. The compared results are given in Table III. It can be seen that the proposed system is obviously better than the existing OWPT systems.

VI. CONCLUSION

In this article, a new MOWPT system is proposed, which can deliver the power to different receivers simultaneously with separate power channels. The key contributions of this article are as follows.

1) The MOWPT system is first proposed. It is based on the *LCL* topology, which has multiple natural resonant angle frequencies and can charge multiple loads simultaneously. Based on the experimental results, the proposed MOWPT system is compared with the OWPT system of other works.
2) The mathematic model of the 0-*LC* MOWPT system is constructed based on the FHA, where the transformers are also taken into consideration. Moreover, the frequency characteristics of this system is analyzed in detail.
3) A parameter design method is proposed, which can be used to design and optimize the MOWPT system.
4) The two power channels are independent, which means the output power of one can be regulated by changing the duty cycle of the corresponding half-bridge inverter.

Accordingly, the experimental results are offered to confirm the validity of the proposed MOWPT system and the parameter design method.

REFERENCES

[1] C. Liu, K. T. Chau, C. Qiu, and F. Lin, "Investigation of energy harvesting for magnetic sensor arrays on Mars by wireless power transmission," *J. Appl. Phys.*, vol. 115, 2014, Art. no. 17E702.

[2] C. Qiu, K. T. Chau, T. W. Ching, and C. Liu, "Overview of wireless charging technologies for electric vehicles," *J. Asian Electr. Veh.*, vol. 12, no. 1, pp. 1679–1685, 2014.

[3] Z. Zhang, K. T. Chau, C. Qiu, and C. Liu, "Energy encryption for wireless power transfer," *IEEE Trans. Power Electron.*, vol. 30, no. 9, pp. 5237–5246, Sep. 2015.

[4] C. Jiang, K. T. Chau, C. Liu, and C. H. T. Lee, "An overview of resonant circuits for wireless power transfer," *Energies*, vol. 10, no. 7, Jun. 2017, Art. no. 894.

[5] Y. Xiao, C. Liu, and F. Yu, "An integrated on-board EV charger with safe charging operation for three-phase IPM motor," *IEEE Trans. Ind. Electron.*, vol. 66, no. 10, pp. 7551–7560, Oct. 2019.

[6] J. Kim, D.-H. Kim, and Y.-J. Park, "Free-positioning wireless power transfer to multiple devices using a planar transmitting coil and switchable impedance matching networks," *IEEE Trans. Microw. Theory Techn.*, vol. 64, no. 11, pp. 3714–3722, Nov. 2016.

[7] M. Fu, T. Zhang, X. Zhu, P. C.-K. Luk, and C. Ma, "Compensation of cross coupling in multiple- receiver wireless power transfer systems," *IEEE Trans. Ind. Inform.*, vol. 12, no. 2, pp. 474–482, Apr. 2016.

[8] Y. Huang, C. Liu, Y. Zhou, Y. Xiao, and S. Liu, "Power allocation for dynamic dual-pickup wireless charging system of electric vehicle," *IEEE Trans. Magn.*, vol. 55, no. 7, Jul. 2019, Art. no. 8600106.

[9] L. Sun, H. Tang, and S. Zhong, "Load-independent output voltage analysis of multiple-receiver wireless power transfer system," *IEEE Antennas Wireless Propag. Lett.*, vol. 15, pp. 1238–1241, 2016.

[10] Y. Zhang, T. Lu, Z. Zhao, F. He, K. Chen, and L. Yuan, "Selective wireless power transfer to multiple loads using receivers of different resonant frequencies," *IEEE Trans. Power Electron.*, vol. 30, no. 11, pp. 6001–6005, Nov. 2015.

[11] F. Liu, Y. Yang, Z. Ding, X. Chen, and R. M. Kennel, "A multifrequency superposition methodology to achieve high efficiency and targeted power distribution for a multiload MCR WPT system," *IEEE Trans. Power Electron.*, vol. 33, no. 10, pp. 9005–9016, Oct. 2018.

[12] F. Liu, Y. Yang, Z. Ding, X. Chen, and R. M. Kennel, "Eliminating cross interference between multiple receivers to achieve targeted power distribution for a multi-frequency multi-load MCR WPT system," *IET Power Electron.*, vol. 11, no. 8, pp. 1321–1328, Jul. 10, 2018.

[13] M. Liu and M. Chen, "Dual-band wireless power transfer with reactance steering network and reconfigurable receivers," *IEEE Trans. Power Electron.*, vol. 35, no. 1, pp. 496–507, Jan. 2020.

[14] Q.-T. Vo, Q.-T. Duong, and M. Okada, "Load-independent voltage control for multiple-receiver inductive power transfer systems," *IEEE Access*, vol. 7, pp. 139450–139461, 2019.

[15] W. Liu, K. T. Chau, C. H. T. Lee, C. Jiang, W. Han, and W. H. Lam, "Multi-frequency multi-power one-to-many wireless power transfer system," *IEEE Trans. Magn.*, vol. 55, no. 7, Jul. 2019, Art. no. 8001609.

[16] V.-B. Vu, V.-T. Phan, M. Dahidah, and V. Pickert, "Multiple output inductive charger for electric vehicles," *IEEE Trans. Power Electron.*, vol. 34, no. 8, pp. 7350–7368, Aug. 2019.

[17] R. Narayanamoorthi, A. V. Juliet, and B. Chokkalingam, "Cross interference minimization and simultaneous wireless power transfer to multiple frequency loads using frequency bifurcation approach," *IEEE Trans. Power Electron.*, vol. 34, no. 11, pp. 10898–10909, Nov. 2019.

[18] X. Dai, X. Li, Y. Li, and A. P. Hu, "Maximum efficiency tracking for wireless power transfer systems with dynamic coupling coefficient estimation," *IEEE Trans. Power Electron.*, vol. 33, no. 6, pp. 5005–5015, Jun. 2018.

[19] R. L. Steigerwald, "A comparison of half-bridge resonant converter topologies," *IEEE Trans. Power Electron.*, vol. 3, no. 2, pp. 174–182, Apr. 1988.

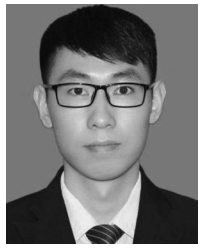

Yongcan Huang (Student Member, IEEE) received the B.Eng. and M.Eng. degrees in control science and engineering from Chongqing University, Chongqing, China, in 2015 and 2018, respectively. He is currently working toward the Ph.D. degree with the City University of Hong Kong, Hong Kong.

His main research interests include power electronics, wireless power transmission, electric vehicle technology, and control of multiphase drive systems.

Chunhua Liu (Senior Member, IEEE) received the B.Eng. and M.Eng. degrees in automatic control from the Beijing Institute of Technology, Beijing, China, in 2002 and 2005, respectively, and the Ph.D. degree in electrical and electronic engineering from the University of Hong Kong, Hong Kong, in 2009.

He is currently an Assistant Professor with the School of Energy and Environment, City University of Hong Kong, Hong Kong. He has authored or coauthored more than 200 refereed papers. His research interests include electric machines and drives, electric vehicles and aircraft, electric robotics and ships, renewables and microgrid, and wireless power transfer.

Dr. Liu is currently an Associate Editor for the IEEE TRANSACTION ON INDUSTRIAL ELECTRONICS, an Editor for the IEEE TRANSACTIONS ON VEHICULAR TECHNOLOGY, and an Editor for the IEEE TRANSACTIONS ON ENERGY CONVERSION. He is a Subject Editor for *IET Renewable Power Generation*, Subject Editor for *Cambridge University Wireless Power Transfer*, an Editor for *Energies*, an Associate Editor for IEEE OPEN JOURNAL OF THE INDUSTRIAL ELECTRONICS SOCIETY, an Associate Editor for the IEEE CHINESE JOURNAL OF ELECTRICAL ENGINEERING, and an Editor for the IEEE TRANSACTIONS ON MAGNETICS—Conference. In addition, he is the Chair and Founder of Hong Kong Chapter, IEEE Vehicular Technology Society.

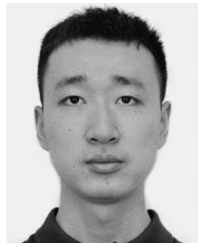

Yang Xiao (Student Member, IEEE) received the B.Eng. degree in electrical engineering and automation from Soochow University, Suzhou, China, in 2014, and the M.Eng. degree in electrical engineering from Southeast University, Nanjing, China, in 2017. He is currently working toward the Ph.D. degree with the City University of Hong Kong, Hong Kong.

His main research interests include power electronics, wireless power transmission, electric vehicle battery charger, and control of multiphase drive systems.

Senyi Liu (Student Member, IEEE) received the B.Eng. and M.Eng. degrees in vehicle engineering from Tongji University, Shanghai, China, in 2015 and 2018, respectively. He is currently working toward the Ph.D. degree with the City University of Hong Kong, Hong Kong.

His main research interests include the advanced control of motor drive systems, electric servo systems, and wireless power transmission.